JIMD-R4 ver.1 220708

Moving towards a novel therapeutic strategy for hyperammonemia that targets glutamine metabolism

Kaori Fukui,[1] Tomoyuki Takahashi,[1,2] Hitomi Matsunari,[3,4] Ayuko Uchikura,[4] Masahito Watanabe[3], Hiroshi Nagashima,[3,4] Naotada Ishihara,[5,6] Tatsuyuki Kakuma,[7] Yoriko Watanabe,[1,8] Yushiro Yamashita,[1] Makoto Yoshino[2]

[1]Department of Pediatrics and Child Health, Kurume University School of Medicine, Kurume, Japan
[2]Division of Gene Therapy and Regenerative Medicine, Cognitive and Molecular Research Institute of Brain Diseases, Kurume University, Kurume, Japan
[3]Meiji University International Institute for Bio-Resource Research, Kawasaki, Japan
[4]Laboratory of Medical Engineering, Meiji University, Kawasaki, Japan
[5]Department of Protein Biochemistry, Institute of Life Science, Kurume University, Kurume, Japan
[6]Department of Biological Sciences, Graduate School of Science, Osaka University, Toyonaka, Japan (present affiliation)
[7]Biostatistics Center, Kurume University, Kurume, Japan
[8]Research Institute of Medical Mass Spectrometry, Kurume University School of Medicine, Kurume, Japan

Correspondence to: Makoto Yoshino, M.D., Ph.D. <yoshino_m@space.ocn.ne.jp>
Division of Gene Therapy and Regenerative Medicine, Cognitive and Molecular Research Institute of Brain Diseases, Kurume University, Asahi-machi 67, Kurume, 830-0011, Japan

Word count: abstract, 249 words; text, 4137 words.

Number of Figures: Four in the text, and one in Supplementary Materials
Number of Tables: None in the text, and two in Supplementary Materials

No color plate requested

Summary

Patients with urea cycle disorders intermittently develop episodes of decompensation with hyperammonemia. Although such an episode is often associated with starvation and catabolism, its molecular basis is not fully understood. First, we attempted to elucidate the mechanism of such starvation-associated hyperammonemia. Using a mouse embryonic fibroblast (MEF) culture system, we found that glucose starvation increases ammonia production, and that this increase is associated with enhanced glutaminolysis. These results led us to focus on α-ketoglutarate (AKG), a glutamate dehydrogenase inhibitor and a major anaplerotic metabolite. Hence, we sought to determine the effect of dimethyl α-ketoglutarate (DKG), a cell-permeable AKG analog, on MEFs and found that DKG mitigates ammonia production primarily by reducing flux through glutamate dehydrogenase. We also verified that DKG reduces ammonia in an NH_4Cl-challenged hyperammonemia mouse model and observed that DKG administration reduces plasma ammonia concentration to 22.8% of the mean value for control mice that received only NH_4Cl. In addition, we detected increases in ornithine concentration and in the ratio of ornithine to arginine following DKG treatment. We subsequently administered DKG intravenously to a newborn pig with hyperammonemia due to ornithine transcarbamylase deficiency and found that blood ammonia concentration declined significantly over time. We determined that this effect is associated with facilitated reductive amination and glutamine synthesis. Our present data indicate that energy starvation triggers hyperammonemia through enhanced glutaminolysis and that DKG reduces ammonia accumulation via pleiotropic mechanisms both *in vitro* and *in vivo*. Thus, cell-permeable forms of AKG are feasible candidates for a novel hyperammonemia treatment.

Synopsis

Cell-permeable α-ketoglutarate is a feasible candidate for a novel hyperammonemia treatment.

CONFLICT OF INTEREST

Kaori Fukui, Tomoyuki Takahashi, Hitomi Matsunari, Ayukuo Uchikura, Masahito Watanabe, Hiroshi Nagashima, Naotada Ishihara, Tatsuya Kakuma, Yoriko Watanabe, Yoshiro Yamashita and Makoto Yoshino declare that they have no conflict of interest.

ANIMAL RIGHTS

All institutional and national guidelines for the care and use of laboratory animals were followed.

AUTHOR CONTRIBUTIONS

Kaori Fukui, Tomoyuki Takahashi and Makoto Yoshino performed *in vitro* and *in vivo* experiments, and drafted manuscript, Hitomi Matsunari and Ayuko Uchikura performed *in vivo* experiments. Naotada Ishihara advised on biochemical analysis. Masahito Watanabe contributed to development of genetically engineered ornithine transcarbamylase-deficient pig model. Hiroshi Nagashima supervised animal experiments and critically appraised the draft. Tatsuyuki Kakuma performed statistical analyses. Yoriko Watanabe performed biochemical analyses. Yushiro Yamashita supervised the drafting process.

Name of corresponding author: Makoto Yoshino, M.D., Ph.D.

FUNDING AFFAIRS

This work was supported by JSPS KAKENHI Grant Numbers JP17K16285 to Kaori Fukui, JP21K07811 to Makoto Yoshino, and AMED Grant Number 19gm0010002h0305 to Hiroshi Nagashima.

KEYWORDS

hyperammonemia - glutaminolysis - anaplerosis - α-ketoglutarate - glutamate dehydrogenase - glutaminase - ornithine transcarbamylase deficiency

AVAILABILITY OF DATA

Data pertinent to the present article are available upon request from the corresponding author, Makoto Yoshino at <yoshino_m@space.ocn.ne.jp>.

1 INTRODUCTION

Patients with urea cycle disorders may develop decompensation with hyperammonemia intermittently. Some such episodes are often associated with starvation, although the events that trigger this type of decompensation are often compounded. As a first-tier measure to treat such decompensation, intravenous administration of hypertonic glucose solution (plus insulin when necessary) and lipid emulsion are recommended to prevent body protein catabolism.[1] However, the molecular basis for hyperammonemia induction by starvation in patients with urea cycle disorders remains to be addressed. The process from body protein degradation to ammonia production involves two steps, namely the degradation of body protein into free amino acids and the subsequent release of ammonia from such amino acids. Free amino acids are either incorporated into body protein or oxidized after they undergo transamination and transfer their amino group onto glutamate.[2] Glutamate is further aminated to form glutamine by glutamate ammonia ligase (GLUL, EC: 6.3.1.2). Glutamine also undergoes γ-deamination by glutaminase to generate glutamate and ammonia. The glutamine degradation pathway is therefore the ultimate exhaust port for amino acid–derived ammonia.

Two glutaminase isoenzymes, namely GLS (EC:3.5.1.2) and GLS2 (EC:3.5.1.2) have been identified. GLS, encoded by *GLS*, is broadly expressed in normal tissue ("kidney-type"); GLS2, encoded by *GLS*2, is expressed primarily in the liver ("liver-type").[3, 4, 5] Glutamate is metabolized to α-ketoglutarate (AKG) by two pathways (Figure 1A).[3] Glutamate is transaminated to asparatate by glutamate oxaloacetate transaminase (GOT). Glutamate is also transaminated to alanine by glutamate pyruvate transaminase isoenzymes GPT1 (EC:2.6.1.3) and GPT2 (EC:2.6.1.7). These transamination reactions do not release ammonia. Glutamate also undergoes oxidative deamination by glutamate dehydrogenase (GLUD), which is associated with ammonia production. Which of the two pathways predominates is determined by a variety of factors, including cell type and glucose availability.[3, 5]

Two glutamate dehydrogenase isoenzymes are known, namely GLUD1 (EC: 1.4.1.3) encoded by *GLUD1* and GLUD2 (EC: 1.4.1.3) encoded by *GLUD*2. GLUD1 is expressed in a variety of tissues, including the liver, while GLUD2 is expressed in neural and testicular tissues.[6] The activities of these enzymes are regulated not only by allosteric effectors but by post-translational modifications exerted by sirtuins located in the mitochondrial matrix, namely SIRT3,[7] SIRT4,[8, 9] and SIRT5.[10, 11, 12, 13] This sequential process whereby the glutamine carbon skeleton feeds the TCA cycle via AKG is called glutaminolysis, a typical anaplerotic reaction, and these are the reactions

that eventually release amino acid–derived ammonia. Herein, we propose a mechanism whereby starvation triggers ammonia production and present the rationale for a strategy to alleviate starvation-induced ammonia production. Moreover, we present evidence that this mechanism as well as some additional mechanism work in animal models of hyperammonemia as well.

2 MATERIALS AND METHODS

2.1 Cell cultures

Mouse embryonic fibroblasts (MEF) stably expressing GFP-LC3 were a gift from Prof. N. Mizushima (The University of Tokyo). We intended to devise an *in vitro* system to measure the ammonia production capacity in isolation by excluding the contribution from ammonia removal. MEF meets this prerequisite because they lack the means to synthesize urea. MEF was first grown overnight in a standard Dulbecco's modified Eagle medium (DMEM) containing 25 mM glucose and 2 mM glutamine but no glutamate. They were later cultured in other media as specified. All cultures were run in duplicate, and the results presented are the means of data from multiple experiments performed on independent occasions. The total number of experiments performed is indicated by "*n*." A dish that contained only cell-free culture medium (cell-free blank) was included in each experiment and ammonia or amino acid concentration values thereof were subtracted from those in test dishes. Metabolite concentration refers to such a net value hereafter unless otherwise specified.

2.2 Determination of ammonia, amino acids, and α-ketoglutarate and calculation of fluxes through glutaminase and glutamate dehydrogenase

Ammonia concentration in the culture medium was measured by an enzymatic method employing bovine liver glutamate dehydrogenase[14] with necessary modifications to allow measurements on a 96-well plate (Supplementary Material 1). In *in vivo* experiments, ammonia concentrations in venous blood or plasma were measured by a microdiffusion method using a PocketChem BA PA-4146^{R} analyzer (Arkray Factory, Koka, Japan). Amino acids in the medium and blood plasma were quantified with an automated amino acid analyzer based on ion exchange column chromatography and post column derivatization with ninhydrin (AminoTac JLC-500/V, Japan Electron

Optics Laboratory, Tokyo, Japan). AKG in plasma was determined using a commercially available kit (α-Ketoglutarate Assay Kit, MAK054, Sigma-Aldrich, St. Louis, U.S.A). We calculated fluxes through GLS, GLUD, and GOT employing values for ammonia and some amino acids, excluding alanine, that exhibited no significant difference between glucose-replete and glucose-starved cultures, according to the following equations[15, 16]: (1) GLS flux = GLUD flux + GOT flux + Δglutamate; (2) GLUD flux = (Δammonia - GOT flux - Δglutamate)/2; and (3) GOT flux = Δaspartate, where Δ denotes the net value of a metabolite's concentration, and the unit for flux is $\mu mol \cdot L^{-1} \cdot 24\ h^{-1} \cdot 1 \times 10^{6}\ cells^{-1}$.

2.3 Quantitative reverse transcription PCR (qRT-PCR)

cDNA was prepared for use in qRT-PCR which was performed on a LightCycler Nano (Roche Diagnostics, Basel, Switzerland) as previously reported.[17] mRNA levels were determined by the $\Delta\Delta C_t$ method and normalized against the level of glyceraldehyde 3-phosphate dehydrogenase (*GAPDH*) mRNA. Primer sequences and temperature conditions employed are shown in Supplementary Material 2.

2.4 Western blotting

Cells were briefly rinsed with ice-cold phosphate-buffered saline (-), scraped off, collected and solubilized in a lysis buffer containing protease and phosphatase inhibitors. Western blotting was performed using rabbit anti-glutamate dehydrogenase 1/2 (D9F7P) mAb, #12793 (Cell Signaling Technology), anti-glutaminase antibody [EP7212] ab 156875 (Abcam), rabbit anti-glutamine synthetase antibody G2781 (Sigma-Aldrich), and mouse anti-GAPDH (clone 6C5) monoclonal antibody (Millipore) as primary antibodies. CFTM 680- or CFTM 770-conjugated goat anti-mouse or rabbit IgG secondary antibodies (Biotium, Hayward, CA, USA) were used as secondary antibodies. Fluorescence emission spectra were acquired and quantified using an Odyssey CLx infrared imaging system (LI-COR Biosciences, Lincoln, NE, USA). For quantitative comparisons, band fluorescence intensities of all of eight specimens were first related to that of specimen 1 for each protein series, including β-actin. These ratios were subsequently normalized to that of β-actin to yield a "relative intensity."

2.5 *In vivo* experiments

We determined whether dimethyl α-ketoglutarate (DKG), a cell-permeable analog of AKG, can alleviate hyperammonemia in animal models. First, we asked whether DKG can reduce hyperammonemia *in vivo* using a NH_4Cl-challenged mouse model.[18] C57BL/6 mice, aged 10 weeks that weighed-21.5±0.5 g, were used. Mice were fed *ad libitum* until 2 h before the experiment and divided into three cohorts, each of which included six mice. The mice were injected intraperitoneally (i.p.) with either saline (cohort 1) or one of the following chemicals dissolved in saline: 10 mmol·kg^{-1} NH_4Cl only (cohort 2), or 10 mmol·kg^{-1} NH4Cl and 5 mmol·kg^{-1} DKG (cohort 3). Blood was obtained by left ventricle centesis under isoflurane inhalation deep anesthesia with a syringe wetted with heparin 30 min after dosing. The blood was subsequently centrifuged at 1,000 *g* for 10 min and plasma was recovered.

We tested the effect of DKG in a male newborn pig with genetically engineered ornithine transcarbamylase deficiency (OTCD).[19, 20] This pig carried a five base-pair deletion (c.186_190delTCTGA) in exon 2 of the *OTC* gene. DKG was first given at 3 h 40 min after delivery as an intravenous (i.v.) bolus at a dose of 1.44 mmol·kg^{-1} diluted in 2 mL of Hartmann's solution containing 5% glucose (HSG), followed by continuous infusion at a rate of 1.44 mmol·kg^{-1}·24 h^{-1} diluted in HSG for the first 4 h. Subsequently, the injected fluid was shifted to the same solution without DKG until the animal was euthanized 9 h into the experiment. This fluid provided 14.4 kCal·kg^{-1}·24 h^{-1}, as glucose. To determine ammonia and AKG levels, blood was drawn at specified time points via the indwelling catheter placed in the superior vena cava under isoflurane anesthesia and analgesia. An aliquot of whole blood was subjected to ammonia determination within 1 min after sampling and plasma was recovered from the remaining blood by centrifugation. Recovered plasma was stored at -30°C until use.

2.6 Statistical analysis

Either one- or two-way analysis of variance (ANOVA) were used to test the significance of effects exerted by experimental factors. ANOVA was followed by either Student's *t*-test or exact Wilcoxon signed rank test for pairwise comparisons. Longitudinal measurements were examined by using mixed effects models. We set $p < 0.05$ as the significance level. Numbers of experiments or mice used (n) as well as statistical methods are given in each subscript.

3 RESULTS

3.1 Glucose starvation enhances ammonia production in cultured mouse embryonic fibroblasts

We first tried to devise an *in vitro* model of energy deficiency–induced ammonia production. The ammonia concentration observed in this experiment represents only the amount of ammonia that is produced. Ammonia removal can be neglected because MEFs cannot synthesize urea. MEFs were cultured in DMEM overnight before being switched to media containing various concentrations of glucose ranging from 0 to 25 mM for an additional 24 h. The ammonia concentration in the culture medium significantly increased at 0 mM glucose compared with 25 mM (Figure 1B). Thus, in the following experiments, cultures in media with either no glucose added or with 25 mM glucose added were used to model energy-starved and energy-replete conditions, respectively.

3.2 Glucose starvation enhances GLS flux and this enhancement contributes to increased ammonia production

Glutaminolysis is the series of biochemical reactions whereby the glutamine carbon skeleton is converted to AKG to feed the TCA cycle. This process culminates in the release of amino acid–derived ammonia (Figure 1A). We hypothesized that glucose starvation-induced ammonia production is associated with enhanced glutaminolysis. We therefore measured glutaminolytic flux to test our hypothesis. When cells were cultured in glucose-starved medium, the ammonia concentration in the medium was higher than for cells cultured in glucose-replete medium (Figure 1C). Most amino acids, including glutamine (Figure 1C), presented negative concentration values (consumed) under both glucose-replete and glucose-starved conditions (Supplementary Material 3). In contrast, glutamate, aspartate, and alanine, the amino acids pertinent to glutaminolysis, presented positive concentration values (secreted) (Figure 1C). We calculated the fluxes through GLS, GLUD, and GOT by employing these values as described in section 2.1. We excluded alanine, however, as it exhibited no significant difference between glucose-replete and glucose-starved cultures. Our calculations indicate that when glucose was replete, the fluxes through GLS and GLUD1 were 306.7 and 205.0 $\mu mol \cdot L^{-1} \cdot 24\ h^{-1} \cdot 1 \times 10^6\ cells^{-1}$, and contributed to 60.0% and 40.0% of total ammonia production, respectively. Under glucose-starved condition, GLS flux significantly increased 1.42 times ($p < 0.05$) and GLUD1 flux exhibited a tendency to increase 1.43 times ($p =$

0.0787), respectively (Figure 1D). Thus, we found that GLS flux contributed to ammonia production in glucose-replete condition. Because we used intact cells in our experiments, the calculated GLS flux represents the apparent flux comprising the activities of some additional factors such as plasma and mitochondrial membrane glutamine transporters as well as cytosolic enzymes, including GLUL. This apparent GLS flux value is expected to approximate that in the whole body.

3.3 Levels of enzymes involved in glutamine metabolism are not significantly affected by glucose starvation

We next determined the transcript levels of three enzymes involved in glutamine metabolism: GLUD1, GLS, and GLUL, in glucose-replete and glucose-starved conditions. The level of *GLUD*1 mRNA was 1.65 times higher under glucose-starved conditions ($p < 0.05$), while there was no significant change in *GLS* and *GLUL* mRNA levels (Figure 2A). In contrast, the protein levels of these enzymes did not change significantly in glucose-starved conditions (Figure 2B). These results suggest that regulation of protein levels is not an important mechanism for controlling the degradation and synthesis of glutamine.

3.4 Patterns of mitochondrial sirtuin expression suggests that sirtuins negatively regulate glutaminolysis

GLS and GLUD1 activities are regulated through post-translational modifications of the enzyme proteins; these modifications are mediated by three mitochondria-associated sirtuins. SIRT3 activates GLUD1,[7] while SIRT4 suppresses GLUD1 in an mTOR-dependent manner.[8, 9] SIRT5 negatively regulates GLS activity by desuccinylation,[10] and stabilizes the enzyme.[11] Fasting has been found to both induce SIRT5[12] and activate GLUD1.[13] In this experiment, *SIRT*3 mRNA levels decreased whereas *SIRT*4 and *SIRT*5 mRNA levels increased under glucose-starved conditions, as opposed to glucose-replete conditions ($p < 0.05$) (Figure 2C). Thus, the expression patterns of *SIRT*3 and *SIRT*4 imply that these sirtuins suppress GLUD1 activity under glucose starvation conditions. Enhanced SIRT5 expression serves to downregulate GLS under glucose-starved conditions although it may also enhance GLUD1 activity.[13] Together, these expression patterns imply that these sirtuins exert, if anything, negative feedback regulation of enhanced glutaminolysis.

3.5 DKG reduces ammonia production mainly by inhibiting GLUD1 activity in cultured mouse embryonic fibroblasts

The results described so far led us to hypothesize that normalization of enhanced glutaminolysis could suppress excessive ammonia production. However, such a suppressive intervention must ensure anaplerosis at the same time because glutaminolysis is a major anaplerotic pathway.[21] We focused on AKG, which is a known inhibitor of GLUD,[6, 22] that meets the two prerequisites. Ammonia production was reduced by the addition of 2 mM DKG in glucose-replete medium, and also by the addition of either 1 mM or 2 mM DKG in glucose-starved medium (Figure 3A). Addition of 2 mM DKG increased the glutamate concentration, irrespective of glucose presence (Figure 3C). Whereas, DKG supplementation at both 1 mM and 2 mM consumed aspartate in glucose-replete as well as glucose-starved cultures, which was suggestive of oxaloacetate anaplerosis (Figure 3D). In contrast, DKG addition did not affect glutamine consumption under both glucose-replete and glucose starved conditions (Figure 3B). To investigate the mechanism whereby DKG reduces ammonia production, we determined the effects of DKG on fluxes through GLS, GLUD1, and GOT. Addition of 2 mM DKG decreased fluxes through all three enzymes compared with the respective control values that received no DKG under both glucose-replete and glucose-starved conditions (Figure 3D, E, F). Such a DKG-induced decrease in flux was more obvious in GLUD1 than in GLS. Notably, the DKG-induced decrease in GLUD1 flux was associated with a concomitant increase in glutamate concentration but was not accompanied by further glutamine consumption (Figure 3B, C). These results indicate that DKG facilitates the reductive amination reaction catalyzed by GLUD1. Furthermore, they suggest that either GLS flux was further checked in part by increased glutamate, a known GLS inhibitor, [4, 23] or that glutamine synthesis was stimulated.

3.6 DKG reduces hyperammonemia in NH_4Cl-challenged mouse model and OTCD newborn pig

We first examined the hyperammonemia-mitigating efficiency of DKG in a mice model. Mice challenged with 10 $mmol \cdot kg^{-1}$ of NH_4Cl i.p.[18] developed a mean plasma ammonia concentration of 4.99 ± 0.32 $mmol \cdot L^{-1}$ (mean ± SD) 30 min after dosing, compared with 0.08 ± 0.01 $mmol \cdot L^{-1}$ in control mice that received saline. When 5 $mmol \cdot kg^{-1}$ of DKG was co-administered with the NH_4Cl dose, the plasma ammonia concentration only reached 1.14 ± 0.28 $mmol \cdot L^{-1}$ (22.8%) (Figure 4A), demonstrating that DKG reduces

plasma ammonia. Plasma glutamate showed a tendency to increase ($p = 0.05838$), but glutamine concentration was not affected by the NH_4Cl challenge. By contrast, alanine, aspartate, arginine, and ornithine concentrations increased (Figure 4A). When DKG was administered along with NH_4Cl, plasma arginine concentration remained unchanged but ornithine concentration increased. Consequently, the ornithine to arginine ratio increased (0.376 ± 0.051 *vs* 0.516 ± 0.042, $p < 0.05$, $n = 6$). These results suggested that in these wild-type mice with normal urea cycle enzymes, ureagenesis was stimulated when they received DKG in addition to NH_4Cl.

Next, we tested if DKG can also mitigate ammonia accumulation in a male newborn pig with hyperammonemia due to OTCD.[19, 20] The newborn pig first received an i.v. bolus of 1.44 $mmol \cdot kg^{-1}$ DKG dissolved in 2 mL Hartmann solution containing 5% glucose (HSG), followed by infusion at a rate of 1.44 $mmol \cdot kg^{-1} \cdot 24\ h^{-1}$ diluted in the same solution for the first 4 h. This solution was designed to supply 14.4 $kCal \cdot kg^{-1} \cdot 24\ h^{-1}$. The fluid was subsequently shifted to HSG alone (Figure 4B). Blood ammonia continued to decline from the pre-DKG value of 171 $\mu mol \cdot L^{-1}$ (wild-type control value: $37.8 \pm 16.0\ \mu mol \cdot L^{-1}$) during the first 4 h while DKG was being infused and following two hours to reach 50.3% of the pre-infusion value at 6 h, and began to rise thereafter. By contrast, plasma AKG level continued to rise while DKG was being infused, and later began to fall, returning to the pre-infusion level 6 h into the experiment. Plasma glutamine and glutamate continued to increase during DKG infusion but began to fall following DKG withdrawal (Figure 4C), indicating that DKG stimulated glutamine synthesis, while plasma alanine and aspartate concentrations decreased with time. Together, DKG was also effective at decreasing ammonia concentration *in vivo*.

4 DISCUSSION

Our study demonstrates that enhancement of glutaminolysis triggers increased ammonia production in energy starvation and it can be alleviated by optimizing glutaminolysis activity. This observation was made in cultured MEFs which cannot synthesize urea. Hence, this result may be applicable to most other organs that do not use the urea cycle. However, *in vivo*, this observation is likely to be modified by the presence of the urea cycle in the liver, the major ammonia removal system.

To determine which of the reactions in the glutaminolysis pathway is induced by glucose-starvation, we calculated fluxes through pertinent enzyme reactions. We thereby found that apparent GLS flux is 1.50 times greater than GLUD1 flux under

glucose-replete conditions. Moreover, we observed that this flux increases by 1.42 and 1.44 times, respectively, when glucose is withdrawn.

We excluded upregulation of expression of the pertinent enzymes both at the level of mRNA and protein as the underlying mechanism. Regulation by post-translational modification of these enzymes would only enable a negative feedback pattern. Together, these enzyme fluxes are likely to be regulated mainly by substrate concentrations, allosteric, and other factors related to GLS,[4, 5] GLUD,[6, 22, 24] and GLUL.[25]

Our study indicates that DKG is effective at reducing ammonia production *in vivo*, as well as *in vitro*. DKG was previously reported to reduce ammonia production in cultured transformed cells.[10, 26, 27] In patients with urea cycle disease, plasma AKG declines in advance of hyperammonemic coma,[28] suggesting that hyperammonemia is prevented to a certain extent by reductive amination at the expense of AKG *in vivo*. However, how this compound works has not been addressed to date. Our flux analyses in this MEF study indicate that both GLS flux and GLUD1 flux were reduced by the addition of 2 mM DKG, and that GLUD1 flux was reduced to a greater extent than GLS flux. In the *in vivo* situation, we expect that GLUD1 flux is similarly affected by DKG as in MEF because this isoenzyme is expressed ubiquitously in various organs, including the liver.[6, 24] At least in the liver, the GLUD1 reaction is now thought to exist in near thermodynamic equilibrium and hence runs in both directions.[5, 6, 29, 30] Hence, any rise in AKG concentration and subsequent decrease in intracellular NAD^+/NADH ratio would favor the reductive amination reaction to form glutamate. The resulting glutamate is further aminated by GLUL to produce glutamine. Both amination reactions consume ammonia.

In our MEF experiments, the concentration of aspartate in the medium was higher in the glucose-depleted culture than in the glucose-replete culture. This result indicates that even under glucose-depleted conditions, the transamination reaction forms aspartate. Which of the two divergent pathways that convert glutamate to AKG is predominantly used reportedly depends on a variety of factors, such as the origin of the cells.[5] Among these factors is glucose availability.[3] This aspartate production may not only serve as a repository of ammonia nitrogen, but to provide cellular building blocks downstream of aspartate that are essential for cellular survival under energy-deprived conditions. Further, DKG addition to the culture media seemed to stimulate reductive amination to form glutamate.

In the same way, the observed changes in plasma glutamate and glutamine concentrations over time in the OTCD pig during DKG infusion indicate that DKG stimulates reductive amination reactions. Additionally, DKG either induces glutamine

synthesis or inhibits its degradation. Meanwhile, plasma concentrations of alanine and aspartate continued to decrease during DKG infusion, which suggests that the transamination pathway had become less active.

In the mouse experiment, plasma alanine and aspartate concentrations increased but the glutamate concentration showed a tendency to increase while glutamine concentrations remained unchanged in the NH_4Cl-challenged cohort compared with the control cohort. These results suggest that the transamination pathways are mostly active in NH_4Cl-challenged mice. Furthermore, in mice administered with both DKG and NH_4Cl, concentrations of glutamate, glutamine, alanine, and aspartate all decreased as compared to mice that received NH_4Cl alone. These data imply that the exogenously loaded ammonia nitrogen was retained as neither glutamine, aspartate, nor alanine. DKG may enhance ureagenesis because both plasma ornithine concentration and the ornithine to arginine ratio increased. By contrast, in MEFs, which do not use the urea cycle, increased ammonia seems to exist mostly in the form of free ammonia and only a minor portion is temporarily retained as glutamate and aspartate. The observations made during these three experiments suggest that DKG may have pleotropic ammonia-reducing activities.

Additional mechanisms may also act to reduce ammonia. A rise in AKG-induced succinyl-CoA flux would increase concomitant GTP production which negatively modulates GLUD.[24] DKG has been reported to promote cellular protein acetylation by increasing cytosolic acetyl-CoA.[31] GLUD1 activity may be negatively regulated by acetylation since GLUD activity increases following deacetylation.[7] DKG has the potential to improve the pathophysiology of hyperammonemic states in other ways. DKG induces anaplerosis not only of AKG but also of oxaloacetate, which would replenish acetyl-CoA. The concept of anaplerotic compensation with appropriate substrates could be applied to the treatment of other diseases characterized by anaplerotic defects such as organic acidemias. Another potential AKG function is either restoring or stimulating protein synthesis, if not both. The mechanistic target of rapamycin complex 1 is known to positively regulate protein synthesis[32] and AKG is an activator of the complex.[33, 34] This leads us to pose two questions: whether hyperammonemia inhibits body protein synthesis (anabolism), and whether AKG can stimulate body protein synthesis regardless of the presence of hyperammonemia.

Our study suggests that DKG is effective in alleviating ammonia accumulation both *in vitro* and *in vivo*. However, there remain several questions to be addressed before AKG, DKG or other analogues can be developed as treatments for hyperammonemia. First, it remains to be determined which of the interactions of DKG

with glutamine metabolism and its anaplerotic effect is the leading mechanism for alleviating or preventing hyperammonemia. Related to this question, it must be determined if DKG administration has an advantage over hypertonic glucose administration, the established first-tier measure for treating hyperammonemia. However, available evidence suggests that DKG has an ammonia-reducing effect that cannot be replaced by glucose and therefore provides an additive therapeutic advantage. In our MEF experiment, DKG addition decreased ammonia concentration in medium irrespective of glucose availability. Additionally, in our OTCD pig experiment, blood ammonia concentration continued to decline while the animal received DKG infusion and began to rise only after DKG infusion was terminated. Furthermore, in the control OTCD pigs that carried the same mutation and received no treatment, blood ammonia increased continuously despite the control pigs receiving more glucose than the pig in the present experiment.[20] Second, ammonia and HCO_3^- are generated from glutamine in the renal proximal tubule, primarily to maintain the acid-base balance of the body's extracellular fluids.[35] Because this is also a major route for ammonia excretion, DKG administration may reduce ammonia disposal from the body. Additionally, the acid-base balance of body fluids may be affected by HCO_3^- produced from administered DKG. Third, in the presence of hyperammonemia, glutamine accumulates in astrocytes, and it may cause astrocyte swelling and eventually lead to brain edema.[36] DKG may increase glutamine concentration within astrocytes if administered after the ammonia concentration in astrocytes has already increased to a certain level. Lastly, it is also important to determine if an AKG salt also works like DKG. An AKG salt can work in theory since Na^+/dicarboxylate cotransporter 3 (NaDC3, *Slc*13*a*3)[37] and an AKG carrier (*Slc*25*a*11)[38] are found on the plasma membrane and mitochondrial membrane, respectively, in various organs including liver and kidney.

Optimization of enhanced glutaminolysis combined with ensured adequate anaplerotic flux to the TCA cycle is a novel and feasible strategy for treating hyperammonemia.

ACKNOWLEDGMENTS

This work was supported by JSPS KAKENHI Grant Numbers JP17K16285 to Kaori Fukui, JP21K07811 to Makoto Yoshino, and AMED Grant Number 19gm0010002h0305 to Hiroshi Nagashima. We would like to express our gratitude to Professor N. Mizushima (Department of Biochemistry and Molecular Biology, Graduate School and Faculty of Medicine, The University of Tokyo) for providing us with MEFs

as well as informative advice on autophagy. We are also grateful to Professor K. Hayasaka (Department of Pediatrics, Yamagata University School of Medicine) for critical comments concerning our study. Lastly, we thank Ms. Kaori Noguchi for her technical assistance.

CONFLICT OF INTEREST

Kaori Fukui, Tomoyuki Takahashi, Hitomi Matsunari, Ayukuo Uchikura, Masahito Watanabe, Hiroshi Nagashima, Naotada Ishihara, Tatsuyuki Kakuma, Yoriko Watanabe, Yushiro Yamashita and Makoto Yoshino declare that they have no conflict of interest.

ORCID Makoto Yoshino https://orcid.org/0000-0001-9048-1490

REFERENCES

1. Häberle J, Burlina A, Chakrapani A, et al. Suggested guidelines for the diagnosis and management of urea cycle disorders: First revision. *J Inherit Metab Dis*. 2019;42(6):1192–1230. doi: 10.1002/jimd.12100.
2. Schutz Y. Protein turnover, ureagenesis and gluconeogenesis. *Int J Vitam Nutr Res.* 2011; 81(2-3):101-107. doi: 10.1024/0300-9831/a000064.
3. Shanware NP, Mullen AR, DeBerardinis RJ, Abraham RT. Glutamine: pleiotropic roles in tumor growth and stress resistance. *J Mol Med.* 2011; 89(3):229-236. doi: 10.1007/s00109-011-0731-9.
4. Katt WP, Lukey MJ, Cerione RA. A tale of two glutaminases: homologous enzymes with distinct roles in tumorigenesis. *Future Med Chem*. 2017; 9(2):223-243. doi: 10.4155/fmc-2016-0190.
5. Altman BJ, Stine ZE, Dang, CV. From Krebs to clinic: glutamine metabolism to cancer therapy. *Nat Rev Cancer*. 2016; 16(10): 619-634. doi: 10.1038/nrc.2016.71.
6. Spanaki C, Plaitakis A. The role of glutamate dehydrogenase in mammalian ammonia metabolism. *Neurotox Res*. 2012; 21(1):117-27. doi: 10.1007/s12640-011-9285-4.
7. Lombard DB, Alt FW, Cheng H-L, et al. Mammalian Sir2 homolog SIRT3 regulates global mitochondrial lysine acetylation. *Mol Cell Biol.* 2007;27(24):8807-8814. doi: 10.1128/MCB.01636-07.
8. Haigis MC, Mostoslavsky R, Haigis KM, et al. SIRT4 inhibits glutamate dehydrogenase and opposes the effects of calorie restriction in pancreatic β cells. *Cell.* 2006;126(5):941-954. doi: 10.1016/j.cell.2006.06.057.

9. Csibi A, Fendt S-M, Li C, et al. The mTORC1 pathway stimulates glutamine metabolism and cell proliferation by repressing SIRT4. *Cell*. 2013;153(4):840-854. doi: 10.1016/j.cell.2013.04.023.
10. Polletta L, Vernucci E, Carnevale I, et al. SIRT5 regulation of ammonia-induced autophagy and mitophagy. *Autophagy.* 2015;11(2):253-270. doi: 10.1080/15548627.2015.1009778.
11. Greene KS, Lukeya MJ, Wang X, et al. SIRT5 stabilizes mitochondrial glutaminase and supports breast cancer tumorigenesis. *Proc Natl Acad Sci. USA.* 2019;116(52): 26625-26632. doi: 10.1073/pnas.1911954116.
12. Buler M, Aatsinki S-M, Izzi V, Uusimaa J, Hakkola J. SIRT5 is under the control of PGC-1 and AMPK and is involved in regulation of mitochondrial energy metabolism. *FASEB J.* 2014, 28(7):3225-3237. doi: 10.1096/fj.13-245241.
13. Wang Y-Q, Wang H-L, Xu J, et al. Sirtuin5 contributes to colorectal carcinogenesis by enhancing glutaminolysis in a deglutarylation-dependent manner. *Nat Commun.* 2018;9(1):545. doi: 10.1038/s41467-018-02951-4.
14. Bergmeyer HU, Beutler H-O (1985）3.3 Ammonia. In Bergmeyer HU. ed. *Methods in Enzymatic Analysis*, 3rd ed., vol VIII. New York: Academic Press, 454-461.
15. Schoolwerth AC, Nazar BL, LaNoue KF. Glutamate dehydrogenase activation and ammonia formation by rat kidney mitochondria. *J Biol Chem.* 1978;253(17):6177-6183. doi: org/10.1016/S0021-9258(17)34596-9.
16. Treberg JR, Clow KA, Greene KA, Brosnan ME, Brosnan JT. Systemic activation of glutamate dehydrogenase increases renal ammoniagenesis: implications for the hyperinsulinism/hyperammonemia syndrome. *Am J Physiol Endocrinol Metab*. 2010; 298(6): E1219–E1225. doi: 10.1152/ajpendo.00028.2010.
17. Hara M, Takahashi T, Mitsumasu C, et al. Disturbance of cardiac gene expression and cardiomyocyte structure predisposes *Mecp2*-null mice to arrhythmias. *Sci Rep.* 2015;5:11204; doi: 10.1038/srep11204.
18. Soria LR, Allegrib G, Melck D, et al. Enhancement of hepatic autophagy increases ureagenesis and protects against hyperammonemia. *Proc Natl Acad Sci USA*. 2018;115(2):391–396. doi: www.pnas.org/cgi/doi/10.1073/pnas.1714670115.
19. Matsunari H, Watanabe M, Nakano K, et al. Modeling lethal X-linked genetic disorders in pigs with ensured fertility. *Proc Natl Acad Sci USA*. 2018; 115(4):70-713. doi: 10.1073/pnas.1715940115.
20. Enosawa S, Hsu H-C, Yanagi Y, Matsunari H, Uchikura A, Nagashima H. Characterization and treatment responsiveness of genetically engineered ornithine

576 transcarbamylase-deficient pig. *J Clin Med.* 2021;10(15):3226. doi:
577 10.3390/jcm10153226.
578 21. Owen OE, Kalhan SC, Hanson RW. The key role of anaplerosis and cataplerosis for
579 citric acid cycle function. *J Biol Chem*. 2002; 277(34):30409-30412. doi:
580 10.1074/jbc.R200006200.
581 22. Smith TJ, Stanley CA. Untangling the glutamate dehydrogenase allosteric
582 nightmare. *Trends in Biochem Sci.* 2008;33(11):557-564. doi:
583 10.1016/j.tibs.2008.07.007.
584 23. Curthoy NP, Watford M. Regulation of glutaminase activity and glutamine
585 metabolism. *Annu Rev Nutr*. 1995;15:133-159. doi:
586 10.1146/annurev.nu.15.070195.001025.
587 24. Plaitakis A, Kalef-Ezra E, Kotzamani D, Zaganas I, Spanaki C. The glutamate
588 dehydrogenase pathway and its roles in cell and tissue biology in health and disease.
589 *Biology.* 2017; 6(1):11. doi:10.3390/biology6010011.
590 25. Bott AJ, Maimouni S, Zong W-X. The pleiotropic effects of glutamine metabolism
591 in cancer. *Cancers.* 2019;11(6): 770; doi:10.3390/cancers11060770.
592 26. Yang C, Sudderth J, Dang T, Bachoo RM, McDonald JG, DeBerardinis RJ.
593 Glioblastoma cells require glutamate dehydrogenase to survive impairments of
594 glucose metabolism or Akt signaling. *Cancer Res.* 2009; 69(20):7986-7993. doi:
595 10.1158/0008-5472.CAN-09-2266.
596 27. Eng CH, Yu K, Lucas J, White E, Abraham RT. Ammonia derived from
597 glutaminolysis is a diffusible regulator of autophagy. *Sci Signal.* 2010;
598 27;3(119):ra31. doi: 10.1126/scisignal.2000911.
599 28. Batshaw ML, Walser M, Brusilow SW. Plasma α-ketoglutarate in urea cycle
600 enzymopathies and its role as harbinger of hyperammonemic coma. *Pediatr Res*.
601 1980; 14(12):1316-1319. doi: 10.1203/00006450-198012000-00008.
602 29. Bailey J, Bell ET, Bell JE. Regulation of bovine glutamate dehydrogenase The
603 effects of pH and ADP. *J Biol Chem.* 1982;257(10):5579-5583. doi:
604 10.1021/bi00567a017.
605 30. Treberg JR, Brosnan ME, Watford M, Brosnan, JT. On the reversibility of glutamate
606 dehydrogenase and the source of hyperammonemia in the
607 hyperinsulinism/hyperammonemia syndrome. *Adv in Enzyme Regul.* 2010;
608 50(1):34-43. doi: 10.1016/j.advenzreg.2009.10.029.
609 31. Mariño G, Pietrocola F, Eisenberg T, et al. Regulation of autophagy by cytosolic
610 acetyl-coenzyme A. *Mol Cell.* 2014; 53(5):710–725. doi:
611 10.1016/j.molcel.2014.01.016.

612 32. Meijer AJ, Lorin S, Blommaart EF, Codogno P. Regulation of autophagy by amino
613 acids and MTOR-dependent signal transduction. *Amino Acids.* 2015; 47(10):2037–
614 2063. doi: 10.1007/s00726-014-1765-4.
615 33. Durán R, Oppliger W, Robitaille AM, et al. Glutaminolysis activates Rag-mTORC1
616 signaling. *Mol Cell.* 2012; 47(3):349–358. doi: 10.1016/j.molcel.2012.05.043.
617 34. Bernfeld E, Menon D, Vaghela V, et al. Phospholipase D–dependent mTOR
618 complex 1 (mTORC1) activation by glutamine. *J Biol Chem.* 2018; 293(42):16390-
619 16401. doi: 10.1074/jbc.RA118.004972.
620 35. Weiner ID and Verlander JW. Renal ammonia metabolism and transport. *Compr*
621 *Physiol*. 2013; 3: 201-220. doi:10.1002/cphy.c120010
622 36. Sørensen M. Update on cerebral uptake of blood ammonia. *Metab Brain Dis*.
623 2013;28:155-9. doi: 10.1007/s11011-013-9395-1.
624 37. Pajor AM. Sodium-coupled dicarboxylate and citrate transporters from the SLC13
625 family. *Pflugers Arch. – Eur. J. Physiol*. 2014;466:119–130.
626 38. Monné M, Miniero DV, Bisaccia F, Fiermonte G. The mitochondrial oxoglutarate
627 carrier: from identification to mechanism. *J. Bioenerg. Biomembr.* 2013;45:1-13.
628
629
630 **Fukui et al., Legend to figures**
631
632 **FIGURE 1** Glucose starvation enhances ammonia production in cultured mouse
633 embryonic fibroblasts and is associated with increased glutaminolytic flux
634
635 A, Glutaminolysis feeds α-ketoglutarate (AKG) into the TCA cycle. Glutamine (Gln) is
636 hydrolyzed by glutaminase (GLS), which releases its γ-amino group, to produce
637 glutamate (Glu). Glu is further metabolized to AKG via two independent pathways. The
638 first pathway is transamination, catalyzed by glutamate oxaloacetate transaminase
639 (GOT) and glutamate pyruvate transaminase (GPT), which happens under glucose-
640 replete conditions. The second is oxidative deamination by glutamate dehydrogenase
641 (GLUD) under glucose starvation conditions. This reaction can be reversible; Glu is
642 regenerated by reductive amination. Glu is also aminated to regenerate Gln by
643 glutamate ammonia ligase (GLUL), a cytosolic enzyme. Ala, alanine; Asp, aspartate;
644 OAA, oxaloacetate and Pyr, pyruvate. Symbols indicate respective atoms: open circles
645 (○), carbons derived from glutamine; closed circles (●), carbons from oxaloacetate or
646 pyruvate; closed squares (■), nitrogen atoms; and α and γ underneath nitrogen atoms
647 represent their origins from α and γ positions of glutamine, respectively.

B, Ammonia concentration normalized by cell count increases as glucose (Glc) concentration falls. Mouse embryonic fibroblasts (MEF) were cultured in DMEM containing glucose at various concentrations as indicated for an additional 24 h after being cultured overnight. Bar charts represent mean ± SEM. Means were compared by one-way ANOVA to determine significant differences; *, $p < 0.05$; **, $p < 0.01$; $n = 4$.
C, Concentrations of ammonia and relevant amino acids under glucose-replete (closed columns) and glucose-starved conditions (open columns). Bar charts represent mean ± SEM. Means were compared by two-way ANOVA to determine significant differences; *, $p < 0.05$; ns, not significant; $n = 3$.
D, Fluxes through glutaminase (GLS), glutamate dehydrogenase (GLUD1) and glutamate oxaloacetate transaminase (GOT) under glucose-replete (closed columns) and glucose-starved conditions (open columns). Flux through GOT is equivalent to the aspartate concentrations. Bar charts represent mean ± SEM. Means were compared by two-way ANOVA to determine significant differences; *, $p < 0.05$; ns, not significant; $n = 3$.

FIGURE 2 Expression levels of enzymes (proteins) pertinent to glutamine metabolism and mitochondria-associated sirtuins under both glucose-replete and glucose-starved conditions

A, Expression levels of mRNA of *GLUD*1, *GLS* and *GLUL* genes, each normalized to glyceraldehyde 3-phosphate dehydrogenase gene (*GAPDH*) expression level. Bar charts represent mean ± SEM. Means were compared by one-way ANOVA to determine significant differences; *, $p < 0.05$; ns, not significant; $n = 3$.
B, Protein levels of GLUD, GLS, and GLUL (bottom, $n = 4$ for each of glucose-replete and glucose-starved cultures). GLUD immunoblot with the first antibody used gives two bands; GLUD1 (lower bands) and GLUD2 (upper bands), respectively. Immunoblot for GLUL also produces two bands, which were summed for quantitative analysis. For quantitative comparison (top), the fluorescence intensity of a given band was normalized to that of β-actin to yield a "relative intensity." Differences were determined by unpaired Student's t-test and exact Wilcoxon signed rank test; ns, not significant; $n = 4$.
C, Levels of *SIRT*3, *SIRT*4 and *SIRT*5 mRNA, each normalized to *GAPDH* mRNA level. Glc, glucose. Bar charts represent mean ± SEM. Means were compared by one-way ANOVA to determine significant differences; *, $p < 0.05$; $n = 3$.

FIGURE 3 DKG reduces ammonia production by inhibiting both GLUD1 and GLS fluxes in cultured mouse embryonic fibroblasts

Concentrations of glucose (Glc) and DKG in culture media are indicated below each column. Data shown in Figure 1D are reproduced in these graphs (columns 25/0 and 0/0) as references. A, ammonia concentration; B, glutamine consumption; C, glutamate secretion; D, changes in aspartate concentration; E, flux through GLS and F, flux through GLUD1. Bar charts represent mean ± SEM. Means were compared by two-way ANOVA; *, $p < 0.05$; **, $p < 0.01$; ns, not significant; $n = 3$.

FIGURE 4 DKG alleviates experimental hyperammonemia in NH_4Cl-challenged mouse and pig with ornithine transcarbamylase deficiency

A, Each of the three cohorts of mice was subjected to intraperitoneal administration with one of the following medications: 1. saline alone (open columns), 2. 10 $mmol \cdot kg^{-1}$ NH_4Cl alone (closed columns), and 3. 10 $mmol \cdot kg^{-1}$ NH_4Cl and 5 $mmol \cdot kg^{-1}$ of DKG (shaded columns). Bar charts represent mean ± SEM. Means were compared by two-way ANOVA to determine significant differences; *, $p < 0.05$; **, $p < 0.01$; ***, $p < 0.001$; $n = 6$ for each cohort.

B, DKG reduces blood ammonia in ornithine transcarbamylase deficiency (OTCD) newborn pig ($n = 1$). This pig carried a five base-pair deletion (c.186_190delTCTGA) in exon 2 of the *OTC* gene. An intravenous bolus of 1.44 $mmol \cdot kg^{-1}$ of DKG dissolved in 2 mL Hartmann solution containing 5% (w/v) glucose (HSG) was first administered (indicated by the closed arrow), at 3 h and 40 min after delivery followed by infusion at a rate of 1.44 $mmol \cdot kg^{-1} \cdot 24\ h^{-1}$ for the first 4 h. Only HSG was infused thereafter. The decline in blood ammonia concentration in the first four hour-period was determined significant as assessed by mixed effects models ($p < 0.001$). Plasma AKG concentration increased along with DKG infusion in the first 4 h period and then began to decline and returned to the pre-infusion level.

C, Plasma glutamine and glutamate continued to increase during DKG infusion, and later began to fall following DKG withdrawal. In contrast, alanine and aspartate continued to decline during the first four hours and afterwards at slower rates.

Supplementary Material 1
Enzymatic determination of ammonia using a 96-well plate

An enzymatic method using glutamate dehydrogenase (Bergmeyer H.U. and Beutler H-O, 1985) was adopted and modified to work on a 96-well plate by generating a standard curve with known amounts of NH_4Cl.

1. Preparation of solutions

1) Solution A
Dissolve 30.22 mg disodium 2-oxoglutarate (Tokyo Chemical Industry, Tokyo, Japan) and 4.1 mg ADP disodium salt (Oriental Yeast, Tokyo) in 10 mL 223.8 mmol/L triethanolamine (TAE) buffer (Fujifilm Wako, Osaka, Japan), adjusted to pH 8.0 with 5 mol/L HCl. Keep on ice until use.

2) Solution B
Dissolve 1.65 mg β-NADH (Oriental Yeast, Tokyo, Japan) in 1 mL 1% $NaHCO_3$ solution. Keep on ice until use.

3) Mix eight parts of Solution A with one part of Solution B (v/v). This mixture is termed "Solution AB."
4) Dilution of GDH enzyme (5x GDH)
Dilute bovine liver GDH (Sigma-Aldrich, Saint Louis, U.S.A., G2626) in Solution AB to provide 12 units of GDH enzyme/mL of assay mixture. This is typically made by diluting one volume of GDH preparation with 4 volumes of Solution AB to prepare "5x GDH." Let the 5x GDH mixture stand on ice until use.
5) Prepare NH_4Cl standard solution to generate a calibration curve.
First dissolve 267.45 mg NH_4Cl (Wako Pure Chemical, Osaka, Japan) in 10 mL double distilled water to prepare 5.0 mmol/L solution. Dilute it with double distilled water to prepare 2.5, 5.0, 7.5, and 10.0 nmol/30 μL solutions. Calibration curve is generated with known amounts of NH_4Cl in each assay because the microplate has some absorbance at 340 nm.

2. Dispensing of solutions and measurement

1) Use Greiner Bio-One UV-Star 96-well microplate. Standards and samples are all measured in duplicate.
2) Dispense 30 μL standard solutions containing 0 (water only, blank), 2.5, 5.0, 7.5, and

10.0 nmol NH_4Cl or 30 µL of appropriately diluted samples into each well.

3) Include 200 nmol/mL NH_4Cl solution as internal control in each assay.
4) Add 90 µL of Solution AB into each well and mix gently by pipetting.
5) Read and record absorbance at 340 nm (A_{340}) on BioTek Synergy HT plate reader (these values are termed "pre-read").
6) Start reaction by adding 5x GDH into wells, mix gently, incubate for 7 minutes at room temperature and read absorbance again ("post-read").

3. Calculation

1) Calculate decrement between the pre-read and post-read values for both samples and standards. This difference is termed "delta read." Subtract blank delta read from both standard and samples.
2) Generate calibration curve using blank-subtracted delta read values for standard solutions and calculate sample concentrations against the generated curve.

4. Results

1) A typical calibration curve is shown below. Concentration of NH_4Cl added to each well and read at A_{340} is linear up to 10.0 nmol of NH_4Cl added. Therefore, samples must be adequately diluted to fall within this range.

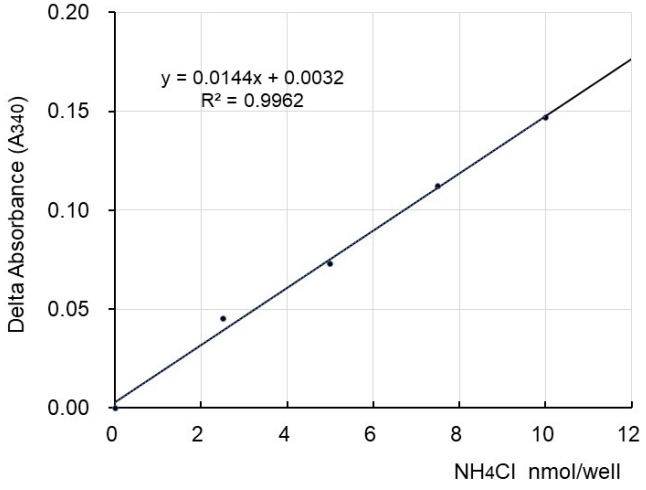

Supplementary Material 2 Primer sequences and thermal cycling conditions for quantitative reverse transcription PCR

Primer names	forward primer (F)	reverse primer (R)	product size (bp)	Reference
mGlud1	5'-CAGGACAGGATATCGGGTGC-3'	5'-TCTCAGGTCCAATCCCAGGT-3'	134	present article
mGls	5'-GGCAAAGGCATTCTATTGGA-3'	5'-TTGGCTCCTTCCCAACATAG-3'	140	present article
mGlul	5'-GCGAAGACTTTGGGGTGATA-3'	5'-CAGTTTGTCAATGGCCTCCT-3'	155	present article
mSirt3	5'-ACAGCTACATGCACGGTCTG-3'	5'-ACACAATGTCGGGTTTCACA-3'	127	Ref. 12
mSirt4	5'-GTGGAAGAATAAGAATGAGCGGA-3'	5'-GGCACAAATAACCCCGAGG-3'	112	Ref. 12
mSirt5	5'-CTCCGGGCCGATTCATTTCC-3'	5'-GCGTTCGCAAAACACTTCCG-3'	136	present article
mGapdh	5'-CCAGAACATCATCCCTGCATC-3'	5'-CCTGCTTCACCACCTTCTTGA-3'	196	Ref. 17

Thermal cycling conditions employed: Denaturation at 98°C for 30 s, annealing at 59°C for 30 s and extension at 59°C for 60 s per cycle, and after 28–30 cycles, further elongation at 72°C for 30 s.

Supplementary Material 3

Effects of glucose availability and dimethyl α-ketoglutarate (DKG) addition on amino acid flux (µmol·L^{-1}·24 hrs^{-1}·1x10^{6} cells, M ± SD)

Glc/DKG (mM)	25/0	25/1.0	25/2.0	0/0	0/1.0	0/2.0
Taurine	-11.87 ±2.59	-10.21 ±6.85	-12.09 ±4.77	-13.13 ±3.46	-14.95 ±2.47	-20.87 ±10.86
Aspartate	-11.87 ±6.44	-10.21 ±6.11	-12.09 ±7.55	-13.13 ±8.57	-14.95 ±9.98	-20.87 ±13.43
Threonine	-82.68 ±37.82	-90.66 ±58.12	-132.66 ±53.54	-171.39 ±45.39	-174.54 ±112.9	-223.62 ±185.53
Serine	-229.00 ±49.85	-207.99 ±71.43	-262.09 ±61.56	-333.69 ±27.62	-342.69 ±104.85	-397.87 ±180.81
Glutamate	84.87 ±42.85	117.66 ±34.45	165.46 ±53.21	109.89 ±11.26	229.43 ±63.28	248.14 ±61.66
Glutamine	-769.16 ±112.40	-645.05 ±200.10	-744.34 ±77.93	-1048.08 ±92.54	-969.68 ±303.54	-922.08 ±350.82
Proline	14.24 ±23.00	2.60 ±18.03	-2.05 ±6.42	17.46 ±10.85	14.42 ±55.38	63.27 ±30.69
Glycine	-42.36 ±13.46	-56.40 ±16.21	-82.11 ±32.17	58.01 ±16.54	69.31 ±24.48	44.75 ±62.47
Alanine	335.21 ±181.36	275.17 ±168.02	317.62 ±167.39	394.58 ±34.05	429.75 ±64.44	458.32 ±95.53
Citrulline	25.01 ±10.07	22.08 ±11.07	21.38 ±13.00	39.00 ±11.85	43.17 ±9.96	46.47 ±7.57
Valine	-157.08 ±55.10	-165.74 ±63.75	-207.93 ±78.1	-260.73 ±45.21	-285.06 ±126.23	-341.64 ±206.98
Cystine	-178.19 ±192.14	-143.06 ±135.14	-203.08 ±205.44	-37.01 ±39.16	-33.02 ±70.92	-44.94 ±87.14
Methionine	-36.55	-38.64	-44.19	-59.76	-61.47	-70.25

	±21.24	±20.75	±22.29	±10.74	±21.51	±32.82
Isoleucine	-209.94	-232.41	-314.35	-352.67	-410.21	-496.39
	±52.65	±60.47	±60.39	±63.05	±124.57	±229.31
Leucine	-241.48	-255.00	-325.18	-397.01	-479.58	-569.97
	±99.79	±95.61	±127.67	±55.48	±144.34	±261.28
Tyrosine	-40.07	-45.79	-52.32	-106.30	-107.19	-117.39
	±26.76	±26.61	±32.29	±15.00	±33.84	±47.07
Phenylalanine	-55.54	-57.05	-60.38	-95.73	-94.97	-105.44
	±33.80	±37.19	±49.57	±10.86	±41.60	±70.90
Ornithine	2.68	0.72	-5.11	-3.62	-5.67	-10.21
	±2.32	±1.28	±2.85	±7.47	±4.14	±4.28
Histidine	-21.53	-26.70	-28.32	-9.01	-21.77	-30.10
	±27.20	±23.89	±28.71	±9.01	±21.77	±30.10
Lysine	-153.58	-144.46	-166.24	-210.54	-240.34	-257.18
	±67.18	±75.17	±87.65	±56.15	±91.63	±132.62
Arginine	-96.80	-92.63	-117.38	-129.37	-136.33	-151.82
	±45.55	±47.13	±50.15	±7.37	±41.86	±85.95